Proceedings of the 7th GACM Colloquium on Computational Mechanics
for Young Scientists from Academia and Industry
October 11-13, 2017 in Stuttgart, Germany

A homogenisation method based on the Irving-Kirkwood-Theory

Maximilian Müller[1]* and Friedrich Gruttmann[1]

Micro Abstract
In this contribution a homogenisation method based on the Irving-Kirkwood theory is introduced. The homogenisation formulas for mass and impulse are consistent with the theory and from there homogenisation formulas for the stress tensor and body force vector are derived. A numerical implementation of the theory is shown and examples with various boundary conditions are presented and compared to results obtained with a Hill-Mandel-approach as well as a full scale approach.

[1]Solid Mechanics, Technical University of Darmstadt, Darmstadt, Germany
***Corresponding author**: mmueller@mechanik.tu-darmstadt.de

Introduction

The existing and in FE^2 widely used Hill-Mandel homogenisation limits possible boundary conditions very strictly. The desire to get rid of those restrictions led to the development of a more general homogenisation method based on the Irving-Kirkwood theory [3]. In this contribution we want to discuss the implementation for small strains and compare results between the new and the Hill-Mandel approach as well as benchmark them with a full scale model.

1 Irving Kirkwood theory

The basis of the Irving Kirkwood theory is a description of the heterogenous body in two scales. One scale shall be a macroscopic one, in which the body is considered to be homogeneous. The homogeneous properties defining the material in the macroscopic scale are extracted through homogenisation from a second, microscopic scale in which the heterogeneous properties of the material are represented.
In detail, there shall be given a body $\mathcal{B}$ inhabiting the area $\mathcal{R}$ with boundary $\partial\mathcal{R}$. A point in $\mathcal{B}$ shall be described with coordinates $\boldsymbol{y}$ defining the macro scale. For very point $\boldsymbol{y}$ there is an assigned surrounding area $\mathcal{P}^{\mathrm{m}}$ of the micro scale, described with coordinates $\boldsymbol{x}$.
For all subdivisions of $\mathcal{R}$ and all $\mathcal{P}^{\mathrm{m}}$ the mass and linear momentum balance laws hold:

$$\dot{\rho}^{\alpha} + \rho^{\alpha}\nabla_y \cdot (\boldsymbol{v}^{\alpha}) = 0, \tag{1}$$

$$\rho^{\alpha}\dot{\boldsymbol{v}}^{\alpha} = \nabla_x \cdot \boldsymbol{\sigma}^{\alpha} + \rho^{\alpha}\boldsymbol{b}^{\alpha}. \tag{2}$$

Here, α is a placeholder for an index m for microscopic or M for macroscopic, indicating the scale in which the quantity is defined. Further, $\nabla_x \cdot (\cdot)$ denotes the divergence of $(\cdot)$ with respect to $\boldsymbol{x}$.
In the next step, the two equations shall be connected as they hold within the same body. For this a homogenisation law is postulated, connecting the density and linear momentum of microscopic and macroscopic scale:

$$\rho^{\mathrm{M}}(\boldsymbol{y}, t) = \int_{\mathcal{R}} \rho^{\mathrm{m}}(\boldsymbol{x}, t) g(\boldsymbol{y}, \boldsymbol{x}) \, \mathrm{d}V^{\mathrm{m}}, \tag{3}$$

$$\rho^{\mathrm{M}}(\boldsymbol{y}, t)\boldsymbol{v}^{\mathrm{M}}(\boldsymbol{y}, t) = \int_{\mathcal{R}} \rho^{\mathrm{m}}(\boldsymbol{x}, t)\boldsymbol{v}^{\mathrm{m}}(\boldsymbol{x}, t) g(\boldsymbol{y}, \boldsymbol{x}) \, \mathrm{d}V^{\mathrm{m}}. \tag{4}$$

In (3) and (4) $g(\boldsymbol{y}, \boldsymbol{x})$ is a weighting function, which needs to fulfill a few basic properties in order to not compromise the theory. For further information on those properties and their implications see [2].
The consistency of these homogenisation laws can be shown by determining the time derivative of (3) and then using only the Reynolds transport theorem, the properties of $g(\boldsymbol{y}, \boldsymbol{x})$ and finally inserting (3) and (4) which leads to the local form of the linear momentum balance (2).
By equal means it can be shown that the homogenisation law for the linear momentum (4) is consistent with the theory as well. From this contemplation we also get a homogenisation law for the stress tensor $\boldsymbol{\sigma}$ and the body force vector $\boldsymbol{b}$:

$$\rho^{\mathrm{M}} \boldsymbol{b}^{\mathrm{M}} := \int_{\mathcal{R}} \rho^{\mathrm{m}} \boldsymbol{b}^{\mathrm{m}} g \, \mathrm{d}V^{\mathrm{m}}, \tag{5}$$

$$\boldsymbol{\sigma}^{\mathrm{M}} := \int_{\mathcal{R}} \left[\boldsymbol{\sigma}^{\mathrm{m}} - \rho^{\mathrm{m}} (\boldsymbol{v}^{\mathrm{m}} - \boldsymbol{v}^{\mathrm{M}}) \otimes (\boldsymbol{v}^{\mathrm{m}} - \boldsymbol{v}^{\mathrm{M}}) \right] g \, \mathrm{d}V^{\mathrm{m}}. \tag{6}$$

In these equations the dependencies of the quantities are left out for better readability.
For a more detailed contemplation on the consistency of (3) and (4), as well as the derivation of (5) and (6) see [2]. Here, a quasi-static case is considered, so the difference in velocity between microscale and macroscale is zero ($\boldsymbol{v}^{\mathrm{m}} - \boldsymbol{v}^{\mathrm{M}} = \boldsymbol{0}$). This leads to a very simple homogenisation law for the stress tensor $\boldsymbol{\sigma}$:

$$\boldsymbol{\sigma}^{\mathrm{M}} := \int_{\mathcal{R}} \boldsymbol{\sigma}^{\mathrm{m}} g \, \mathrm{d}V^{\mathrm{m}}. \tag{7}$$

2 Finite element formulation

From now on, we want to limit the theory to small strains and set the weighting function to $g(\boldsymbol{y}, \boldsymbol{x}) = \frac{1}{V^{\mathrm{m}}}$, where V^{m} is volume of the representative volume element (RVE). In order to get rid of the restrictions on the boundary conditions in the Hill-Mandel theory, an additional constraint connecting microscopic and macroscopic strains is introduced:

$$\boldsymbol{\epsilon}^{\mathrm{M}} = \int_{\mathcal{R}} \boldsymbol{\epsilon}^{\mathrm{m}} g \, \mathrm{d}V^{\mathrm{m}} = \frac{1}{V^{\mathrm{m}}} \int_{\mathcal{R}} \boldsymbol{\epsilon}^{\mathrm{m}} \, \mathrm{d}V^{\mathrm{m}} \qquad \Leftrightarrow \qquad \int_{\mathcal{R}} (\boldsymbol{\epsilon}^{\mathrm{M}} - \boldsymbol{\epsilon}^{\mathrm{m}}) \, \mathrm{d}V^{\mathrm{m}} = 0. \tag{8}$$

This additional constraint shall be introduced into the weak form of equilibrium via 6 Lagrange multipliers for the 6 equations resulting from (8) for each RVE. We vary with respect to the displacements $\boldsymbol{u}$, the Lagrange multipliers $\boldsymbol{\mu}$ and the macroscopic strains $\boldsymbol{\epsilon}^{\mathrm{M}}$. The latter allows a much easier formulation of the homogenisation and implementation into the existing FE code than the approach presented in [3]. With vanishing boundary and body volume forces, this leads to:

$$\int_{\mathcal{R}} \delta\boldsymbol{\epsilon}^{\mathrm{mT}} \boldsymbol{\sigma}^{\mathrm{m}} - \delta\boldsymbol{u}^{\mathrm{T}} \boldsymbol{f} \, \mathrm{d}V^{\mathrm{m}} + \int_{\mathcal{R}} \delta\boldsymbol{\mu}^{\mathrm{T}} (\boldsymbol{\epsilon}^{\mathrm{M}} - \boldsymbol{\epsilon}^{\mathrm{m}}) \, \mathrm{d}V^{\mathrm{m}} + \int_{\mathcal{R}} \boldsymbol{\mu}^{\mathrm{T}} (\delta\boldsymbol{\epsilon}^{\mathrm{M}} - \delta\boldsymbol{\epsilon}^{\mathrm{m}}) \, \mathrm{d}V^{\mathrm{m}} = 0. \tag{9}$$

Linearisation and a standard iso-parametric FE-formulation leads to:

$$L[\dots] = \delta\boldsymbol{V}^{\mathrm{mT}} (\boldsymbol{K}\Delta\boldsymbol{V}^{\mathrm{m}} + \boldsymbol{A}\Delta\boldsymbol{\mu} + \boldsymbol{F}) + \delta\boldsymbol{\mu}^{\mathrm{T}} (\boldsymbol{A}^{\mathrm{T}}\Delta\boldsymbol{V}^{\mathrm{m}} + \boldsymbol{T}\Delta\boldsymbol{\epsilon}^{\mathrm{M}}) + \delta\boldsymbol{\epsilon}^{\mathrm{MT}} (\boldsymbol{T}^{\mathrm{T}}\Delta\boldsymbol{\mu}) = 0. \tag{10}$$

Where $\boldsymbol{\epsilon}^{\mathrm{m}} = \boldsymbol{B}\boldsymbol{V}^{\mathrm{m}}$, $\boldsymbol{K}$ is the stiffness matrix and $\boldsymbol{V}^{\mathrm{m}}$ the displacement vector for the RVE. The matrices $\boldsymbol{A}$ and $\boldsymbol{T}$ are defined below.

$$\boldsymbol{K} := \int_{\omega} \boldsymbol{B}^{\mathrm{T}} \boldsymbol{D} \boldsymbol{B} \, \mathrm{d}V^{\mathrm{m}}, \quad \boldsymbol{A} := -\int_{\omega} \boldsymbol{B}^{\mathrm{T}} \, \mathrm{d}V^{\mathrm{m}}, \quad \boldsymbol{T} := \int 1 \, \mathrm{d}V^{\mathrm{m}}. \tag{11}$$

In matrix form:

$$\begin{bmatrix} \delta\boldsymbol{V}^{\mathrm{m}} \\ \delta\boldsymbol{\mu} \\ \delta\boldsymbol{\epsilon}^{\mathrm{M}} \end{bmatrix}^{\mathrm{T}} \left\{ \begin{bmatrix} \boldsymbol{K} & \boldsymbol{A} & \boldsymbol{0} \\ \boldsymbol{A}^{\mathrm{T}} & \boldsymbol{0} & \boldsymbol{T} \\ \boldsymbol{0} & \boldsymbol{T} & \boldsymbol{0} \end{bmatrix} \begin{bmatrix} \Delta\boldsymbol{V}^{\mathrm{m}} \\ \Delta\boldsymbol{\mu} \\ \Delta\boldsymbol{\epsilon}^{\mathrm{M}} \end{bmatrix} + \begin{bmatrix} \boldsymbol{F} \\ \boldsymbol{0} \\ \boldsymbol{0} \end{bmatrix} \right\} = 0. \tag{12}$$

We now subdivide the displacement vector for each element $\boldsymbol{v}_e$ into a free part $\boldsymbol{v}_\mathrm{f} = \boldsymbol{a}_e \boldsymbol{V}^\mathrm{m}$ and a part with boundary conditions $\boldsymbol{v}_\mathrm{b} = \boldsymbol{M}_e \Delta\boldsymbol{\epsilon}^\mathrm{M}$, where $\boldsymbol{a}_e$ is the standard assembly operator and $\boldsymbol{M}_e$ is defined below:

$$\boldsymbol{v}_e = \begin{bmatrix} \boldsymbol{v}_\mathrm{f} \\ \boldsymbol{v}_\mathrm{b} \end{bmatrix} = \begin{bmatrix} \boldsymbol{a}_\mathrm{e} & \boldsymbol{0} \\ \boldsymbol{0} & \boldsymbol{M}_e \end{bmatrix} \begin{bmatrix} \boldsymbol{V}^\mathrm{m} \\ \Delta\boldsymbol{\epsilon}^\mathrm{M} \end{bmatrix}, \tag{13}$$

where: (14)

$$\boldsymbol{M}_e = \begin{bmatrix} \vdots \\ \boldsymbol{M}_I \\ \vdots \end{bmatrix} \quad \text{and } \boldsymbol{M}_I = \begin{bmatrix} X_{I1} & 0 & 0 & X_{I2} & X_{I3} & 0 \\ 0 & X_{I2} & 0 & X_{I1} & 0 & X_{I3} \\ 0 & 0 & X_{I3} & 0 & X_{I1} & X_{I2} \end{bmatrix}. \tag{15}$$

Here, I denotes the nodes with boundary conditions. So $\boldsymbol{M}_e$ has as many rows as there are boundary conditions.
Inserting this into (12) and subdividing the corresponding matrices $\boldsymbol{K}$ and $\boldsymbol{A}$, leads to:

$$L[g(\dots)] = \begin{bmatrix} \delta\boldsymbol{V}^\mathrm{m} \\ \delta\boldsymbol{\epsilon}^\mathrm{M} \\ \delta\boldsymbol{\mu} \\ \delta\boldsymbol{\epsilon}^\mathrm{M} \end{bmatrix}^\mathrm{T} \left\{ \begin{bmatrix} \boldsymbol{K}_\mathrm{ff} & \boldsymbol{K}_\mathrm{fb} & \bar{\boldsymbol{A}}_\mathrm{f} & \boldsymbol{0} \\ \boldsymbol{K}_\mathrm{bf} & \boldsymbol{K}_\mathrm{bb} & \bar{\boldsymbol{A}}_\mathrm{b} & \boldsymbol{0} \\ \bar{\boldsymbol{A}}_\mathrm{f}^\mathrm{T} & \bar{\boldsymbol{A}}_\mathrm{b}^\mathrm{T} & \boldsymbol{0} & \boldsymbol{T} \\ \boldsymbol{0} & \boldsymbol{0} & \boldsymbol{T} & \boldsymbol{0} \end{bmatrix} \begin{bmatrix} \Delta\boldsymbol{V}^\mathrm{m} \\ \Delta\boldsymbol{\epsilon}^\mathrm{M} \\ \Delta\boldsymbol{\mu} \\ \Delta\boldsymbol{\epsilon}^\mathrm{M} \end{bmatrix} + \begin{bmatrix} \boldsymbol{F}_\mathrm{f} \\ \boldsymbol{F}_\mathrm{b} \\ \boldsymbol{0} \\ \boldsymbol{0} \end{bmatrix} \right\} = 0. \tag{16}$$

Implementation into a multi-scale FE formulation follows standard procedure as is described e.g. in [1]. The derivation of the homogenised stiffness matrix and stress resultants for each Gauss point also follows the same procedure as shown in [1].
As a remark on the implementation, it shall be noted, that for $\boldsymbol{\mu}$ and $\boldsymbol{\epsilon}^\mathrm{M}$ we introduced four additional nodes into every RVE, which are then part of every element in that RVE. While the nodes carrying the Lagrange multipliers $\boldsymbol{\mu}$ are left unbound, the ones carrying $\boldsymbol{\epsilon}^\mathrm{M}$ are fully bound and internally loaded with their respective values.

3 Numerical Examples

3.1 RVE boundary conditions

Several RVE displacement boundary conditions were tested, following the ones proposed in [3]. Here, we will only use two of them. The first one, referred to as RB1, is a minimal configuration which constrains only the rigid body motions of the RVE. The second one, referred to as RB2, is a Hill-Mandel like boundary condition that fully constrains all nodes on all outer boundaries of the RVE. In RB2 the corner nodes had to be released from all boundary conditions, in order to allow a numerical solution as the system of equations would have been overdetermined otherwise.

3.2 Bending of inhomogeneous beam

The implemented homogenisation method was first tested on a homogeneous tension rod and on a homogeneous beam in bending to varify basic functionality. The results obtained were exactly the same as the results obtained with a Hill-Mandel approach and a full scale model with solid 3d elements. The results were independent from the chosen RVE boundary condition.
Next, we tested an inhomogeneous beam, that consisted of a soft matrix material and cube shaped inclusions, that were a hundred times stiffer than the matrix material. the cubes made up one ninth of the overall volume (see figure 1).
The results showed a slightly stiffer response for the RB2 configuration compared to RB1. The results of the Hill-Mandel homogenisation were very close to the ones of the RB2 configuration. The full scale model with only 1 inhomogeneity per cross section was significantly softer than both coupled models. The full scale model with 2 inhomogeneities per cross section showed a response very close to the one of the RB1 configuration. Results for a model with 3 inhomogeneities per cross section could not be obtained as the inversion of the stiffness matrix exceeded the system's memory.

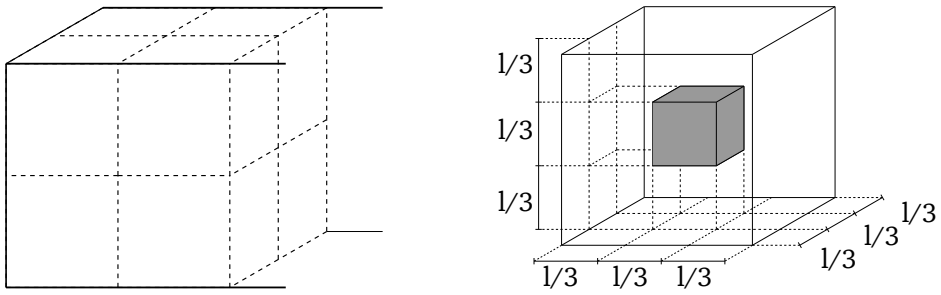

Figure 1. Full scale model of the beam (left) with 2x2 blocks of inhomogeneities (dashed) in the cross section and one such block on the right (also a depiction of the RVE)

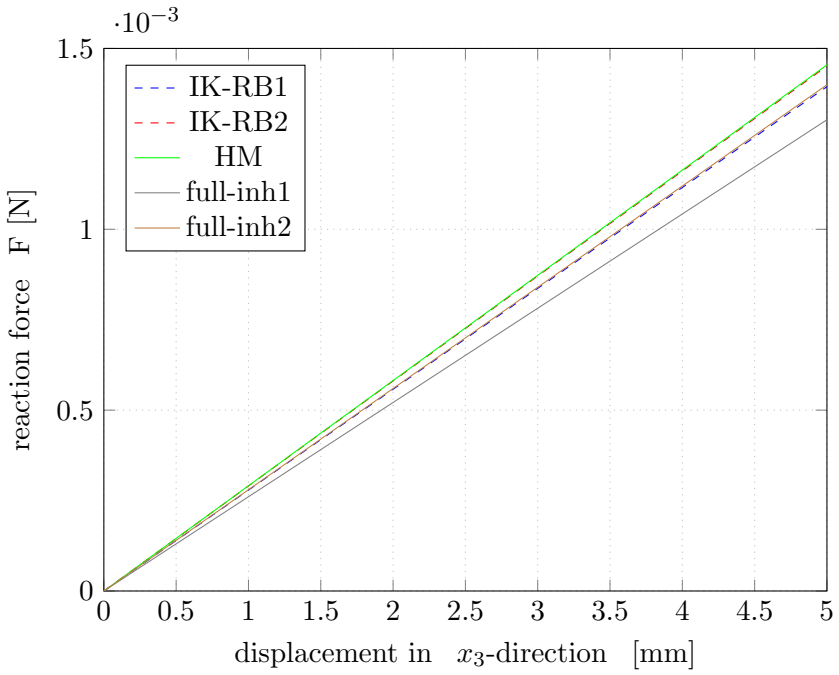

Figure 2. Reaction force over displacement for a cantilever with a single force on the free end, compared are Irving-Kirkwood homogenisation (IK) with two different boundary conditions with a Hill-Mandel homogenisation (HM) and a full scale modell with 1 (inh1) and 2 (inh2) inhomogeneities per cross section

References

[1] F. Gruttmann and W. Wagner. A coupled two-scale shell model with applications to layered structures. *International Journal for Numerical Methods in Engineering*, 94:p. 1233–1254, 2013.

[2] K. K. Mandapu, A. Sengupta, and P. Papadopoulos. A homogenization method for thermo-mechanical continua using extensive physical quantities. *Proceedings of the Royal Society*, 468:p. 1696–1715, 2012.

[3] B. S. Mercer, K. K. Mandapu, and P. Papadopoulos. Novel formulations of microscopic boundary-value problems in continuous multiscale finite element methods. *Computer Methods in Applied Mechanics and Engineering*, 286:p. 268–292, 2015.